

Article

A New Real-Time Pinch Detection Algorithm Based on Model Reference Kalman Prediction and SRMS for Electric Adjustable Desk

Minming Gu ¹, Yajie Wei ¹, Haipeng Pan ^{1,*} and Yujia Ying ²

¹ Faculty of Mechanical Engineering & Automation, Zhejiang Sci-Tech University, Hangzhou 310018, China; guminming@zstu.edu.cn (M.G.); 2018g0507020@mails.zstu.edu.cn (Y.W.)

² Nanhu College, Jiaxing University, Jiaxing 314001, China; yyj@zjxu.edu.cn

* Correspondence: pan@zstu.edu.cn

Received: 15 July 2020; Accepted: 13 August 2020; Published: 20 August 2020



Abstract: This paper presents a new algorithm based on model reference Kalman torque prediction algorithm combined with the sliding root mean square (SRMS). It is necessary to improve the accuracy and reliability of the pinch detection for avoiding collision with the height adjustable desk and accidents on users. Motors need to regulate their position and speed during the operation using different voltage by PWM (Pulse Width Modulation) to meet the requirement of position synchronization. It causes much noise and coupling information in the current sampling signal. Firstly, to analyze the working principle of an electric height adjustable desk control system, a system model is established with consideration of the DC (Direct Current) motor characteristics and the coupling of the system. Secondly, to precisely identify the load situation, a new model reference Kalman prediction method is proposed. The load torque signal is selected as a pinch state variable of the filter by comparing the current signal. Thirdly, to meet the need of the different loads of the electric table, the sliding root means square (SRMS) of the torque is proposed to be the criterion for threshold detection. Finally, to verify the effectiveness of the algorithm, the experiments are carried out in the actual system. Experimental results show that the algorithm proposed in this paper can detect the pinched state accurately under different load conditions.

Keywords: anti-pinch detection; model reference adaptive kalman prediction; sliding root mean square (SRMS); height adjustable desk

1. Introduction

People spend quite a large portion of their day-time in sedentary behavior [1]. With the continual increase of sitting down hours, musculoskeletal system problems are becoming more and more serious [2]. For the sake of alleviating this problem, the electric height adjustable desk is widely used in today's office worldwide [3]. Automatically adjusting the height of the desk using DC (Direct Current) motors provides an alternative working pattern to choose standing or sitting. Meanwhile, it also brings some safety problems during its rising or falling. Children or careless people may injure themselves when they misuse a height adjustable desk. Thus, during the movement, the state must be monitored and diagnosed effectively to guarantee safe operation and prevent human casualties. Therefore, anti-pinch detection is an essential function in the adjustable height desk and plays a crucial role in reliable operation.

Many researchers have conducted intensive research on anti-pinch detection. In pinch detection of car window, which is similar to the height adjustable desk, angular velocity detection [4,5], armature current detection [6–9], torque rate detection [10–12], and torque detection [13–15] of the motor are

often used. As the armature current value and motor torque of DC motor are reflected in the running state, those threshold values are selected as a basis for judgment [7]. When the desk meets obstacles during the rising or falling process, current or torque value exceeds the threshold, and the window begins to retract. Unfortunately, it has a poor performance in the real system. As the desk should keep the position synchronization of different desk legs, the cross-coupling between motors [16] will be obvious. Meanwhile, compared with windows, the PWM (Pulse Width Modulation) signal of motor speed regulation will also introduce noise. To make up for the inadequateness in the practical situation, choosing the appropriate filtering algorithm is the key.

There exist various kinds of filter design, such as H_∞ filter [17,18], H_-/H_∞ filter [19], Kalman filter [20,21], particle filters [22,23], fast Fourier transform (FFT) [24,25], wavelet transform (WT) [26–29], empirical mode decomposition (EMD) [30,31], independent component analysis (ICA) [32], and so on. H_∞ filter does not make an assumption about the noise, and it minimizes the maximum estimation error, but H_∞ filter cannot guarantee that the pinch system's estimation error is minimized owing to its high computational cost [33]. Particle filtering shows obvious superiority in processing the nonlinear state-space model [34]. Particle filtering uses Monte Carlo simulation to achieve recursive Bayesian filter by a large number of random samples called particles. The core is to use a group of random samples (particles) with corresponding weights to represent the posterior distribution of states, and the weighted sum of random samples is used as estimates of states. Filter design lacks the analysis of the input interference signals, which easily leads to deviations and divergences in the estimates. Owing to its multi-resolution properties and behavior of singularities [29], wavelet transform can locate the particular points and widely used in many domains. However, wavelet transform needs a high operating cost for real-time detection. For electric height adjustable desk pinch detection, the filter method not only should be intelligible to be compatible with different load conditions, but should also have low computational costs. Among these algorithms, the Kalman filter has a lower calculation and is suitable for real-time detection. The Kalman filter is mainly used to estimate system states that can only be observed indirectly or inaccurately by the system itself [35].

On the other hand, the fixed absolute pinch estimator used in the car window [13] is not suitable for our plant. It does have a fast response and is easy to implement. However, the load over the height adjustable desk is uncertain and would be changed anytime. The fixed value cannot distinguish the actual load situation. It might not be a general solution because the plants would easily miss the pinch and make false alarms. A variable threshold will be able to distinguish the situation of the pinch better.

In this paper, the electric height adjustable desk system, which uses sampling resistors as the current detection sensor of the motor, has adopted a new real-time pinch detection algorithm based on model reference Kalman prediction and dynamic threshold using sliding root mean square (SRMS). In this algorithm, the mathematical and simulation model is established to present the relationship between the DC motor load torque and input variables, which contains current signals, voltage, and noises. Moreover, the armature voltage is given by the based on the cross-coupling control. Then, the load torque estimation based on the steady-state Kalman filter is presented. The motor parameter identification [36] is conducted to improve the performance of the steady-state Kalman filter. The SRMS of pinch torque is used as the anti-pinch criterion, which not only quickly identifies the anti-pinch points of different load states, but also has strong robustness under different working conditions.

2. Model of Electrical Height Adjustable Desk

The electric height adjustable desk is commonly driven by two permanent magnets brushed DC motors (PMDC). For a DC motor drive system, there are two essential balance equations, including voltage and torque balance equation in model. The voltage balance equation can be expressed as follows:

$$L \frac{dI_d}{dt} = U_d - I_d R - E_a \quad (1a)$$

$$E_a = K_e * \omega \quad (1b)$$

The torque balance equation can be expressed as follows:

$$J \frac{d\omega}{dt} = T_c - T_l - T_\mu + \mu_v \tag{2a}$$

$$T_c = K_t * I_d \tag{2b}$$

$$T_l = T_{load} + T_p \tag{2c}$$

$$T_\mu = B_\mu * \omega \tag{2d}$$

In Equation (2c), T_l is subdivided into T_{load} and T_p . T_{load} is the load torque, which is used to drive load in a normal condition of an electric height adjustable desk. T_{load} is proportional to the weight of the load. T_p is the pinch torque that only appears when obstacles hinder the raising and lowering of the height adjustable desk. As the vibration torque μ_v varies during its operating condition, it can be assumed as a zero-mean white noise input u_{μ_v} with the variance Q_{μ_v} .

On the basis of the above balance equations, I_d and ω are selected as the state variables. The state-space model of DC motor can be expressed as follows:

$$\begin{cases} \dot{x} = Ax + Bu + w \\ y = Cx + v \end{cases} \tag{3}$$

where

$$A = \begin{bmatrix} -\frac{R}{L} & -\frac{K_e}{L} \\ \frac{K_t}{J} & -\frac{B_\mu}{J} \end{bmatrix}, B = \begin{bmatrix} \frac{1}{L} & -\frac{1}{J} \end{bmatrix}^T, C = [1 \ 0]^T$$

$$x = [I_d \ \omega]^T, u = [U_d \ T_l]^T, w = [0 \ \mu_v]^T$$

Here, w is the plant noise of the height adjustable desk system and v is the measurement noise of a height adjustable desk system. U_d is armature voltage, which is a time variable. It is the output of the following controller, which contains the PWM signal.

There are two motors in the mentioned height adjustable desk, for dual motor position synchronization problem, a cross-coupling control strategy is introduced to solve the dual-motor synchronization problem. The position bias between the two motors uses a cross-coupling control strategy based on PID (Proportion Integration Differentiation) control to compensate for the synchronous position error. The dual-motor position control method of the height adjustable desk system is shown in Figure 1. In the block diagram, for each motor, the error between the target position and real position is the input of the position PID controller. The PID controller is used to regulate the duty cycle of the PWM generator. The trigger signal PWM of power generator drive H-bridge to generate the armature voltage U_d , which is used to drive each motor. For dual-motor, there is a bias between real position 1 and 2. The bias as the cross-coupling controller compensates and diminishes the synchronous position error.

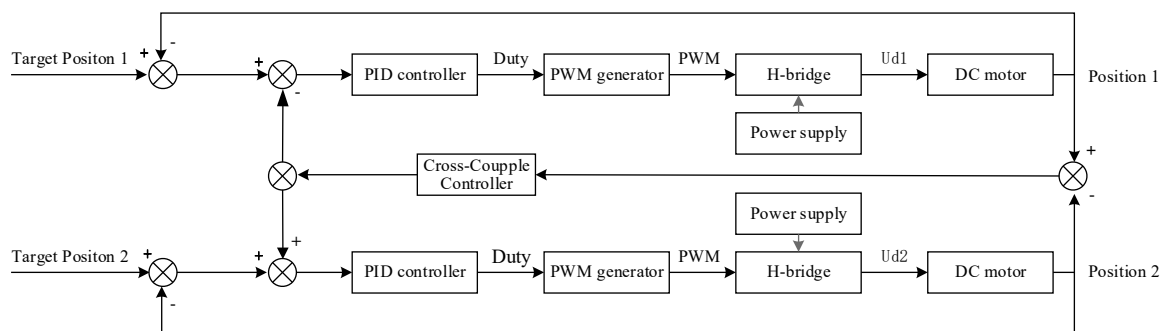


Figure 1. The control block diagram of the height adjustable desk system.

3. The Steady-State Kalman Filter Based Pinch Torque Estimation

In this section, pinch torque estimation based on the steady-state Kalman filter is presented. At the beginning of pinch torque estimation, pinch state variables should be selected correctly. Then, the Kalman filter is introduced. Besides, for linear time-invariant systems, the steady-state Kalman filter can replace with traditional Kalman filter to save computational resources. Finally, the flow of pinch detection based on the Kalman filter is presented.

3.1. Selecting State Variable for Pinch Detection

In the height adjustable desk system, there are so many state variables that can be selected as pinch detection state variables to detect pinch condition, such as armature current, current rate, motor angular velocity, angular velocity rate, motor torque, and torque rate. Torque and torque rate are less sensitive to the motor parameter. Moreover, it is more straightforward to select motor torque as a pinch detection state variable to detect pinch conditions. However, torque cannot be measured directly. To solve the above problem, state estimation with the Kalman filter is used to predict torque. The traditional torque estimation method is based on control torque as follows:

$$T_c = (U_d - K_e * \omega) \frac{K_t}{L_s + R} \quad (4)$$

Because the electrical dynamics of the motor is much faster than the mechanical one, the control torque of the motor can be expressed as follows:

$$T_c \approx \frac{(U_d - K_e * \omega)}{R} * K_t = K_t * I_d \quad (5)$$

From Equation (5), it can be seen that T_c is proportional to armature current, which is equivalent to estimate armature current. Owing to the impact of dual motor synchronization, the amplitudes of oscillation of the armature current ripple are amplified, which makes it difficult to judge whether the height adjustable desk is encountering obstacles. The measured armature currents when encountering obstacles shown in Figure 2.

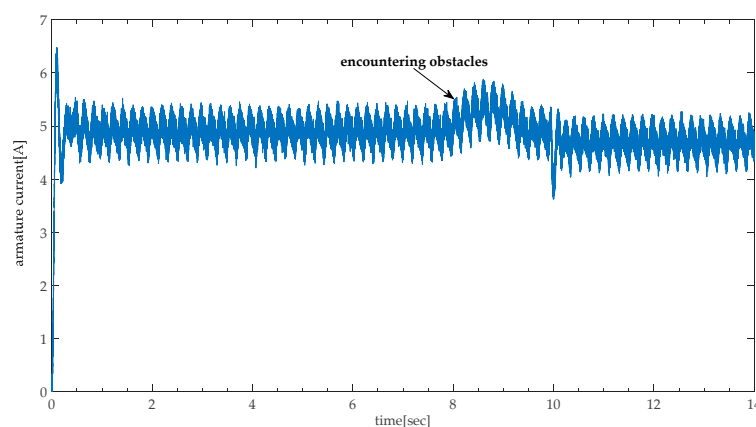


Figure 2. The curve of armature current when encountering obstacles.

From Equation (2a–d), the following equation can be obtained:

$$T_l = T_{load} + T_p = K_t * I_d - J * \dot{\omega} - B_\mu * \omega + \mu_v \quad (6)$$

In Equation (6), T_{load} is used to drive the initial load, which varies with the initial load. T_p only appears when the height adjustable desk encounters obstacles. Thus, T_l is selected as the pinch state variable. As shown in Figure 3, T_l calculated by Equation (6) can present the change of load and the situation of encountering obstacles in height adjustable desk. Furthermore, it can be seen that the

estimation of T_l relies on the estimation of I_d and ω . In the next section, the state-space model for pinch detection will be established based on the steady-state Kalman filter.

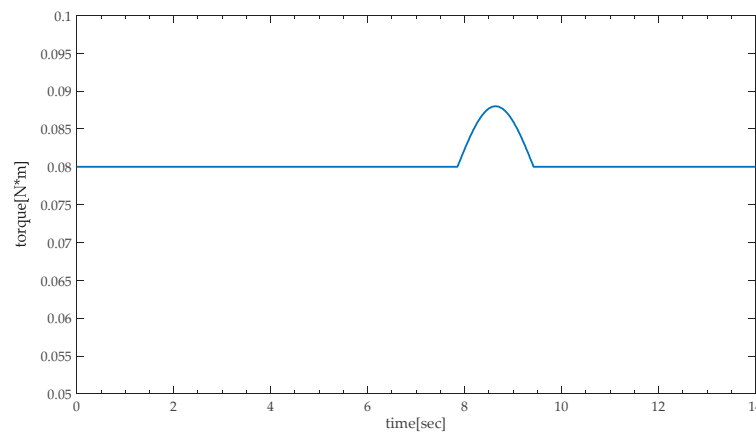


Figure 3. Load torque curve including initial load and encountering obstacles.

3.2. The Steady-State Kalman Filter Based Pinch Detection

In this section, pinch detection of the height adjustable desk based on the steady-state Kalman filter is designed to detect pinch state. From the above Section 3.1, T_l is selected as the pinch state variable. According to [10,11], it is reasonable to augment the torque T_l as an additional state and modeled by a random walk using the zero-mean white noise μ_T with the variance Q_T as follows:

$$\dot{T}_l(t) = \mu_T(t) \quad (7)$$

The state-space model can be expressed as follows:

$$\begin{cases} \dot{x} = Fx + Gu + w \\ y = Hx + v \end{cases} \quad (8)$$

where

$$x = [I_d \ \omega \ T_l]^T, \ u = U_d, \ y = I_d, \ w = [0 \ \mu_v \ \mu_T]^T$$

$$F = \begin{bmatrix} -\frac{R}{L} & -\frac{K_e}{L} & 0 \\ \frac{K_t}{J} & -\frac{B_\mu}{J} & -\frac{1}{J} \\ 0 & 0 & 0 \end{bmatrix}, \ G = \begin{bmatrix} \frac{1}{L} \\ 0 \\ 0 \end{bmatrix}, \ H = \begin{bmatrix} 1 \\ 0 \\ 0 \end{bmatrix}$$

Let the process noise and the observation noise be uncorrelated. $w(k)$ is the process noise that is assumed to be drawn from a zero-mean multivariate normal distribution with covariance $Q(k)$, which $\mu_v(k)$ meets the Gaussian white noise with zero-mean and variance q_v , and $\mu_T(k)$ the Gaussian white noise with zero-mean and variance q_T . Similarly, the observation noise $v(k)$ meets the Gaussian white noise with zero-mean and variance $R(k)$.

Before the pinch observer design, it is necessary to prove the observability of (8), the judgment matrix of the observability is presented as follows:

$$\text{rank} = \begin{bmatrix} H \\ HF \\ HF^2 \end{bmatrix} = \begin{bmatrix} 1 & 0 & 0 \\ -\frac{R}{L} & -\frac{K_e}{L} & 0 \\ X_1 & X_2 & \frac{K_e}{L*J} \end{bmatrix} \quad (9)$$

where

$$X_1 = \frac{R^2}{L^2} - \frac{K_e * K_t}{L * J}, \ X_2 = \frac{K_e * R}{L^2} + \frac{B_\mu * K_e}{L * J}$$

It is evident that the rank is 3, which means that the state-space Equation (8) can be observed. Thus, the armature current is suitable to be estimated and is used to estimate state variable T_l .

To facilitate the above design in discrete time, it is necessary to discretize the state-space model. Using a sampling period T_s , the state-space model can be rewritten as follows:

$$\begin{aligned} x(k+1) &= \Phi x(k) + \Gamma u(k) + w(k) \\ y(k) &= Hx(k) + v(k) \end{aligned} \quad (10)$$

where

$$\Phi = e^{FT_s}, \quad \Gamma = (e^{FT_s} - I)F^{-1}G$$

For simplification to be achieved, using the backward difference to make some approximation, they can be written as follows:

$$\begin{aligned} \Phi &= e^{FT_s} \approx FT_s + I \\ \Gamma &= (e^{FT_s} - I)F^{-1}G \approx GT_s \end{aligned}$$

Then, Equation (10) can be expressed as follows:

$$\begin{bmatrix} I_d(k+1) \\ \omega(k+1) \\ T_l(k+1) \end{bmatrix} = \begin{bmatrix} 1 - \frac{R}{L} * T_s & -K_e * \frac{T_s}{L} & 0 \\ \frac{K_t * T_s}{J} & 1 - \frac{B}{J} * T_s & -\frac{T_s}{J} \\ 0 & 0 & 1 \end{bmatrix} * \begin{bmatrix} I_d(k) \\ \omega(k) \\ T_l(k) \end{bmatrix} + \begin{bmatrix} \frac{T_s}{L} \\ 0 \\ 0 \end{bmatrix} * U_d + \begin{bmatrix} 0 \\ \mu_v \\ \mu_T \end{bmatrix} * T_s \quad (11)$$

After discretization is completed, the Kalman filter is introduced to modify and update the state variables. It is generally known that useful information is always affected by white noise in a real physical system. In this case, the Kalman filter is designed to minimize the variance of the estimation error. The standard Kalman filter consists of two parts: the predict step and update step.

For linear time-invariant systems (system matrices are not varying with time), the posteriori estimation error covariance matrix $P(k|k)$ and the prior estimation error covariance matrix $P(k|k-1)$ will converge towards steady-state values, which can be pre-calculated. Taking account of the real-time implementation issue, the steady-state Kalman filter gain is used. The steady-state estimation error covariance matrix P_∞ holds the following discrete-time algebraic Riccati equation:

$$P_\infty = \Phi \left[P_\infty - P_\infty H^T (HP_\infty H^T + R)^{-1} HP_\infty \right] \Phi^T + Q \quad (12)$$

Then, $K(k)$ can be replaced with K_∞ holding the following equation:

$$K_\infty = P_\infty H (HP_\infty H^T + R)^{-1} \quad (13)$$

Thus, the above five equations about the Kalman filter can be simplified into two equations:

$$\hat{x}(k|k-1) = \Phi(k)\hat{x}(k-1|k-1) + \Gamma(k)u(k) \quad (14a)$$

$$\hat{x}(k|k) = \hat{x}(k|k-1) + K_\infty(y(k) - H(k)\hat{x}(k|k-1)) \quad (14b)$$

4. Threshold Design and Judgment Criteria of Pinch Condition

After the pinch torque is estimated, the remaining problem in pinch detection is to determine the threshold level of the torque. To observe the estimated torque data in Figure 4, avoiding the start-up phase of the motor, it can be seen that the torque has a certain distribution characteristic during the stable condition. The quantile–quantile plot is used to check the normality of the torque data. The result is shown in Figure 5. The quantile–quantile plot uses quantiles as the standard for evaluating the normality. If the data completely conform to the normal distribution, the scattered points form a straight line in the figure; the closer the scattered points are to the straight line, the better

the normality. From Figure 5, the normality of the torque performs well. Thus, it is reasonable to use the confidence zone method to judge whether the obstacles are pinched [37].

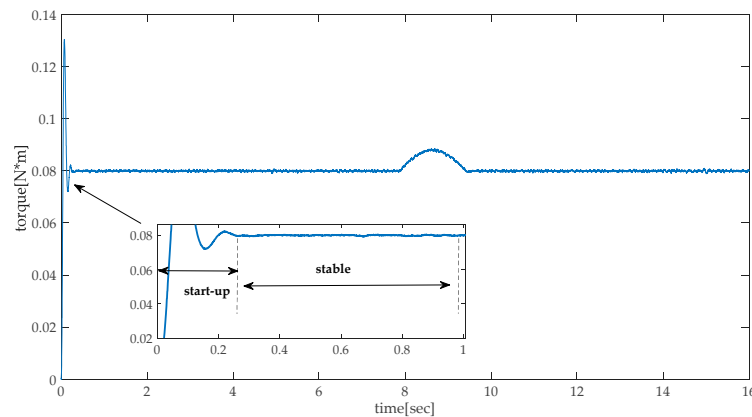


Figure 4. Estimated torque curve of the electric height adjustable desk's running process.

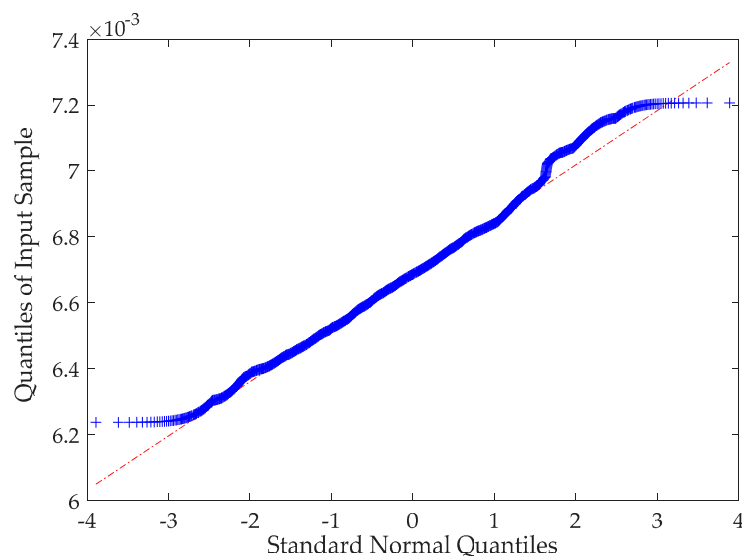


Figure 5. The quantile–quantile plot of the estimated torque data.

To determine the torque's confidence zone, firstly, obtaining the mean value μ_T of the torque in stable condition, m and n correspond to the end moment t_m and the start moment t_n of stable conditions, respectively.

$$\mu_T = \frac{1}{m-n+1} \sum_{j=n}^m T_j \quad (15)$$

Then, to get the standard deviation of the torque in stable condition,

$$\sigma_T = \left[\frac{1}{m-n} \sum_{j=n}^m (T_j - \mu_T)^2 \right]^{\frac{1}{2}} \quad (16)$$

According to the related knowledge of the normal distribution, the 99.73% confidence zone of the torque can be expressed as follows:

$$\Psi_T = [\mu_T - 3 * \sigma_T, \mu_T + 3 * \sigma_T] \quad (17)$$

Ψ_T probably describes the range of possible changes of the torque when the height adjustable desk is on stable condition. In the case of the stable condition of the height adjustable desk, it is almost sure that the motor torque value will not exceed the confidence zone. Thus, the prescribed threshold can be set as T_{th} .

$$T_{th} = \mu_T + 3 * \sigma_T \quad (18)$$

On the other hand, because the plant noise and observer noise exist during the height adjustable desk operation, if the prescribed threshold is compared with the estimated torque, there will be a misjudgment of pinch condition. Using the method of sliding root mean square with the estimated torque, the sliding root mean square can be expressed as follows:

$$T_M = \frac{1}{l_m} \sqrt{\sum_{j=M-l_m+1}^M T_j^2} \quad (19)$$

l_m is the window length value of the sliding, which can be determined according to the actual situation. In our application, $l_m = 16$.

Let the smoothed torque T_M compare with the prescribed threshold T_{th} , when T_M is greater than T_{th} , the anti-pinch function of the height adjustable desk starts, which reverses the motor to release obstacles.

5. Pinch Detection Experiments

In this section, an electric height adjustable desk platform is given. Then, the dual-motor position synchronization algorithm is verified in MATLAB, which is consistent with the actual control method, as shown in Figure 1. On the basis of dual-motor synchronization, the pinch detection method proposed in this paper is verified with MATLAB. The simulation is conducted under a slight and heavy load situation. In addition, the actual experiment is implemented to validate the performance of the height adjustable desk pinch detection algorithm proposed in this paper.

5.1. Simulation Conditions

To validate the performance of the proposed method, the simulations are given with MATLAB. Considering the plant noise caused by the power supply and PWM in practice, and the measurement noise v is introduced into the simulations, where the plant noise w and the measurement noise v conform to a zero-mean, with a Gaussian distribution with variance Q and variance R , respectively. They can be replaced by uncorrelated white noise. The motor parameters are obtained by the recursive least squares (RLS) in Table 1.

Table 1. Motor parameters.

Symbols	Values	Unit
Power supply	12	V
L	0.0709	H
R	1.17	Ω
K_e	0.0178	V/rad/s
K_t	0.0178	N·m/A
J	4.0×10^{-6}	Kg·m ²
B_μ	1.9×10^{-5}	Kg·m ²

Owing to the coupling synchronization of two motors, there are mutual influences on their speed and armature current, which makes it hard to detect the pinch condition using them as pinch detection variables. Before the pinch detection, it is necessary to verify the synchronization between the two motors. As shown in Figure 6, there is a difference in the initial load of the two motors. Under the effect of cross-coupling control, dual motors achieve position synchronization. It can be seen that the torque

increases distinctly when the height adjustable desk pinching obstacles, but the speed and current reflect the changes indirectly. That consolidates and verifies the accuracy of selecting the torque as a pinch detection state variable. In Figure 6, ‘position 1’ and ‘position 2’ represent the position of the two motors. ‘est’ and ‘true’ represent estimation results and simulation results of the model calculation mixed with the system noise, respectively.

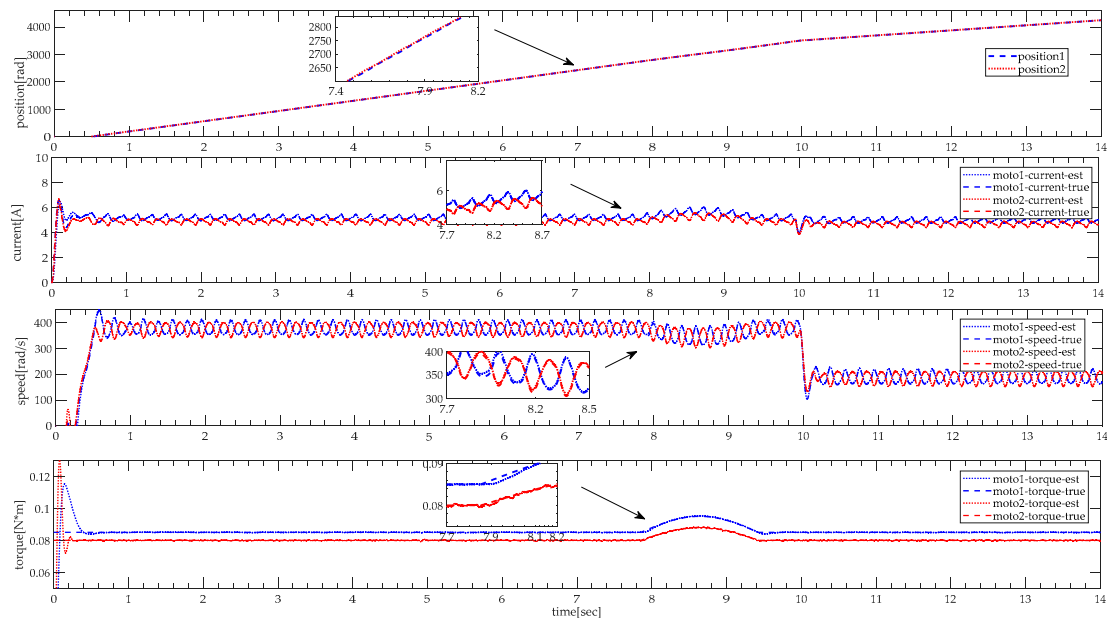


Figure 6. Status information under dual-motor position synchronization.

On the basis of the position synchronization of dual motors, in order to validate the performance of the height adjustable desk pinch detection algorithm proposed in this paper, the simulation experiments are implemented consisting of slight and heavy loads. According to the standards of the electric lifting desk industry, the pinch force must not exceed 100 N. In practice, the screw lead L of the height adjustable desk is generally 20 mm. The transmission efficiency η is 90%. The gear ratio i is 44:1. The relationship between screw thrust F and torque can be expressed as follows:

$$F * L = 2 * \pi * torque * i * \eta \quad (20)$$

In our simulation experiments, the max load is set as 80 kg, which needs 800 N to drive. According to the above relationship between screw thrust and torque, the needed torque is about 0.064 N·m. Thus, 100 N is equal to 0.008 N·m. The pinching force can be simulated as follows:

$$F_P = 0.008 \sin(\pi * t) \quad t \in [2.5\pi, 3\pi] \quad (21)$$

The simulation experiments are implemented under a slight and heavy load situation, which slight load is set under 30 kg (about 0.024 N·m), and heavy load of 80 kg (about 0.064 N·m). In practice, there is a different load to drive between moto 1 and moto 2. Thus, there exists a bias in loads. In the heavy load situation, the angular velocity, the armature current, and the torque of motor 1 and 2 are illustrated in Figures 7 and 8. As shown in Figures 7 and 8, when the height adjustable desk pinches the obstacles in heavy load, angular velocity slightly decelerates, and the armature current slightly increases as well. However, it can be seen that torque distinctly increases, and torque does not fluctuate like the angular velocity and armature current. In contrast, as shown in Figures 9 and 10, when the obstacles are pinched by the height adjustable desk in a slight load, the angular velocity also slightly decelerates, but the armature current and torque change more obviously, armature current abruptly

increases, and torque sharply rises. The simulation results show that the pinch detection algorithm can detect the pinch state regardless of a heavy load or light load.

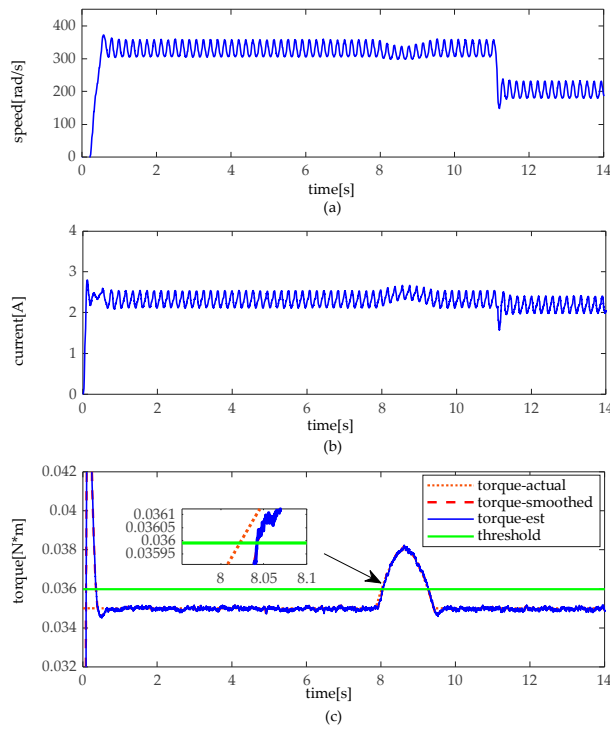


Figure 7. Pinch detection results of moto 1 in heavy load. (a) angular velocity. (b) armature current (c) pinch detection with torque.

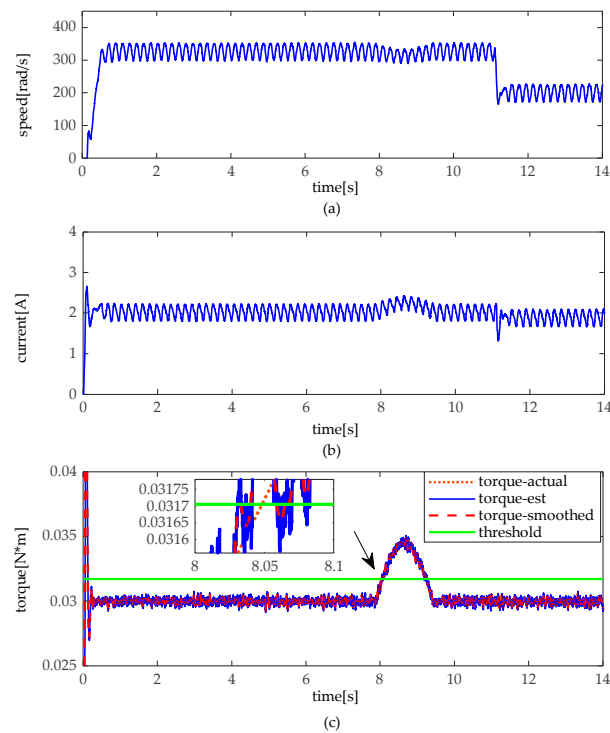


Figure 8. Pinch detection results of moto 2 in heavy load. (a) angular velocity. (b) armature current (c) pinch detection with torque.

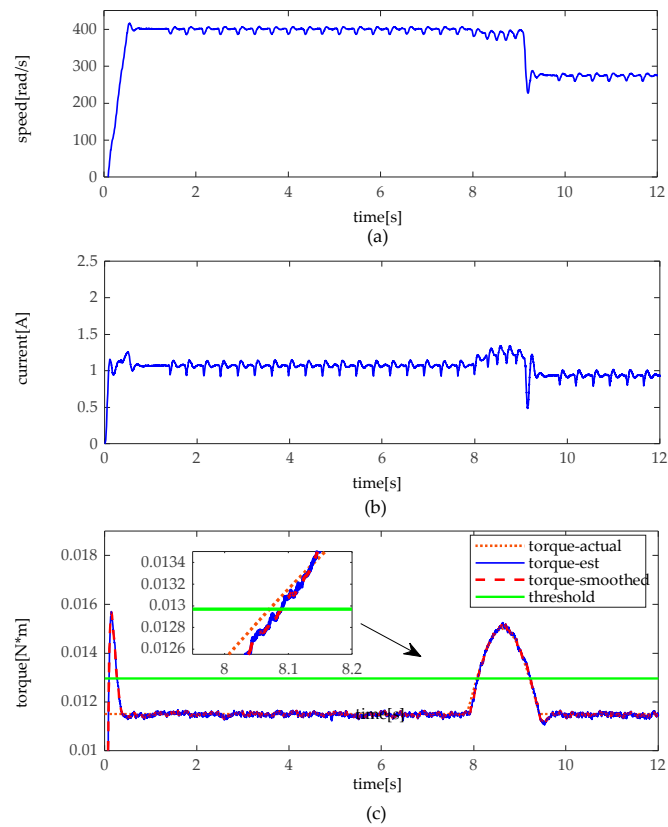


Figure 9. Pinch detection results of moto 1 in slight load. (a) angular velocity. (b) armature current (c) pinch detection with torque.

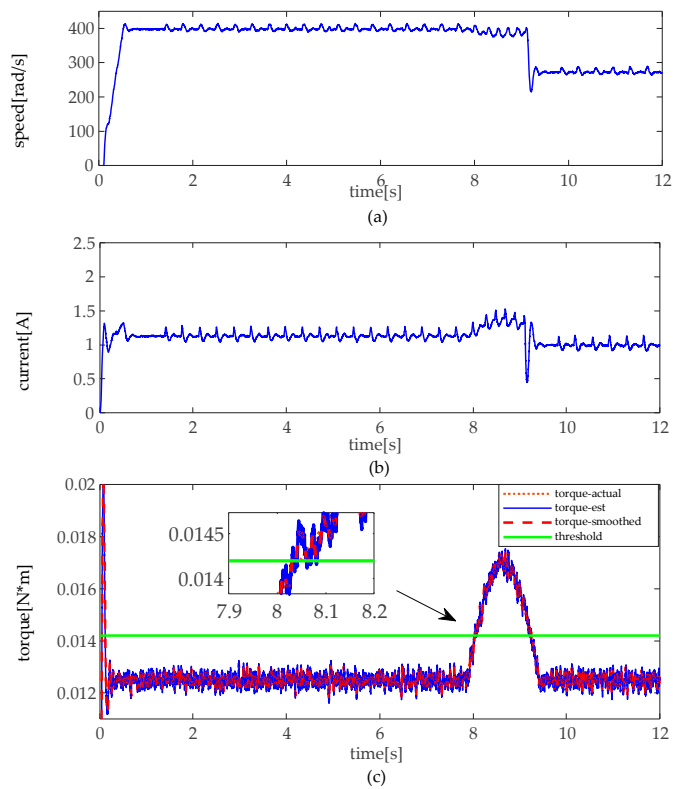


Figure 10. Pinch detection results of moto 2 in slight load. (a) angular velocity. (b) armature current (c) pinch detection with torque.

5.2. Experimental Verification

The electric height adjustable desk test platform and control system structure are adopted in this paper to validate the performance of the proposed method, as shown in Figures 11 and 12. In this platform, a DC power is supplied to the whole platform. The SIRIUS data acquisition instrument collects the motor armature currents and armature voltages with a 20 kHz sampling rate. The collected data observed by the SIRIUS are stored on the host computer. These collected data are used to estimate the torque. Two hall sensors are used to measure the height of the desk. Two sampling resistors are used to detect motor armature current. The STM32F103C8T6 produced by S.T. is selected as the control chip. The electric height adjustable desk is equipped with a separate lifting DC motor at each leg. Though a special motor drive chip, the control signal from STM32 is used to control the electric lifting desk movement.

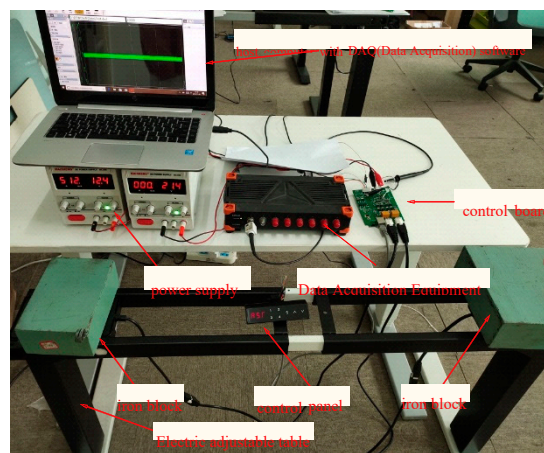


Figure 11. Electric adjustable desk.

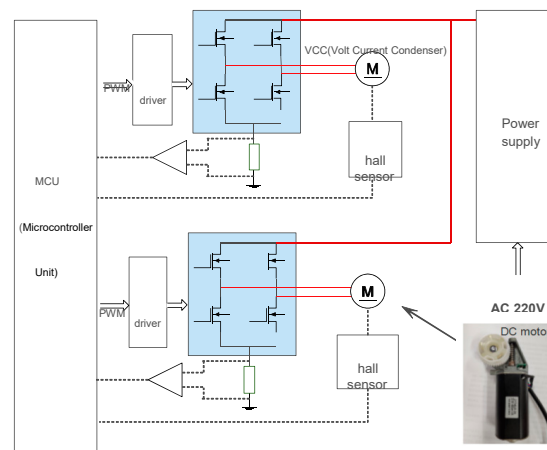


Figure 12. The control system structure.

In practice, the experiments are conducted in two situations, rising and lowering. As shown in Figure 13, there is an abrupt change of armature current and torque during the rising of the height adjustable desk when the desk pinches the obstacle. Figure 13b shows that the smoothed torque is greater than the threshold at about 6.6 s, which can trigger the motor's retracting to release the obstacle. As shown in Figure 14, the torque effect will be less than 0 during the lowering of the desk owing to the effect of gravity. However, when the obstacle appears, there will be positive torque. The above simulation and experiment indicate that the pinch detection algorithm proposed in this paper can successfully detect the pinch condition.

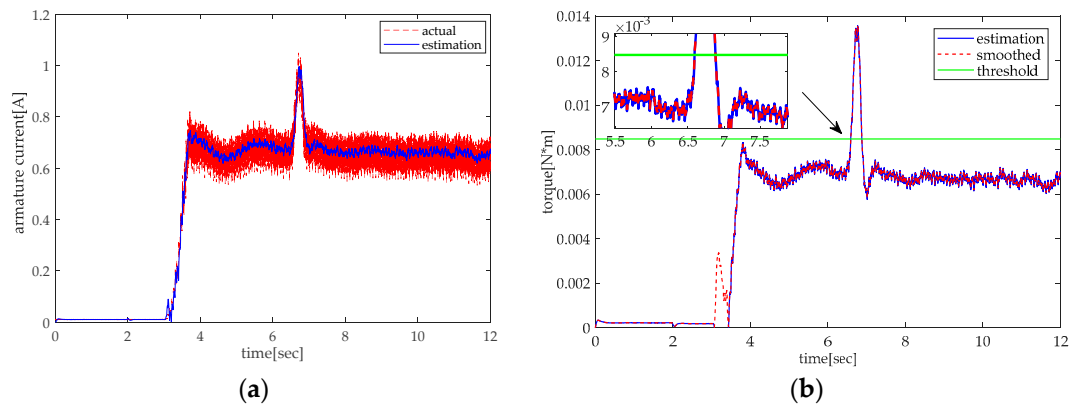


Figure 13. Pinch detection of the rising experiment: (a) armature current and (b) pinch detection with torque.

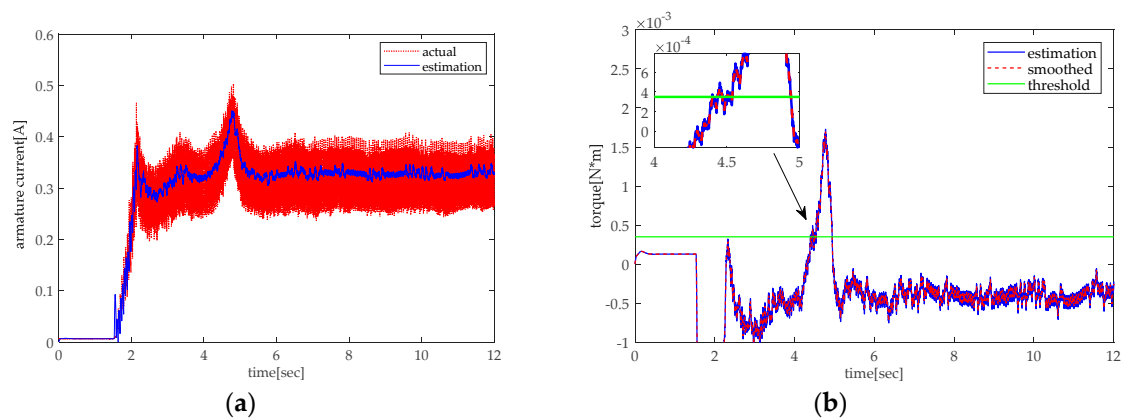


Figure 14. Pinch detection of the lowering experiment: (a) armature current and (b) pinch detection with torque.

6. Conclusions

A new algorithm based on the model reference Kalman torque prediction algorithm combined with the sliding root mean square (SRMS) is proposed to conduct the pinch detection of the electric height adjustable desk. To implement pinch detection, the system model is established by DC motor dynamics. Considering the position synchronization of the dual-motor, the cross-coupling control strategy is introduced into the system model. To eliminate the influence of dual motor synchronization and noise from PWM, a new pinch state variable for pinch detection is proposed and compared with the traditional pinch state variable. To save computational cost in MCU (Microcontroller Unit), the steady-state Kalman filter is introduced to estimate the pinch state variable. To improve the performance of the steady-state Kalman filter, the motor parameter is obtained by RLS. To judge pinch state, the sliding root means square method combined with the confidence zone is used to determine the dynamic threshold.

The simulations and experiments show that the electric height adjustable desk pinch detection method can successfully detect the pinch condition in different situations. Moreover, the proposed pinch detection algorithm can recognize pinch state under different loads. The proposed pinch detection method will improve the reliability and safety of the current electric adjustable desk anti-pinch function.

7. Patents

1. China Patent Application, CN 201910508440.0. A kind of electric adjustable desk resistance detection method and control device.

- China Patent Application, CN **201811374738.9**. Gesture recognition and position adjustment device for the electric adjustable desk.

Author Contributions: M.G. and Y.W. conceived and designed the experiments, they together wrote the manuscript. M.G. proposed the idea of the analysis method. Y.W. designed the embedded software, performed parts of experiments, and analyzed the data. H.P. was the project administration and organized the structure of this paper. Y.Y. reviewed and edited the manuscript. All authors have read and agreed to the published version of the manuscript.

Funding: This research was funded by “Zhejiang Science Technology Department Public Service Technology Research Project” (grant number LGG19F030002”) and the “Fundamental Research Funds of Zhejiang Sci-Tech University” (grant number 2019Q032).

Acknowledgments: Thanks to Shaoxing Contuo Transmission Technology co. Ltd. for offering the electric adjustable desk, and we would like to thank all of the anonymous reviewers spent their own time to review and give the suggestions.

Conflicts of Interest: The authors declare no conflict of interest.

Nomenclature

L	Armature inductance
I_d	Armature current
R	Armature resistance
U_d	Armature voltage
E_a	Motor back electromotive force
K_e	Back electromotive force constant
K_t	Torque constant
ω	Angular velocity
J	Moment of inertia
B_μ	Viscous friction constant
T_c	Control torque
T_{load}	Load torque
T_p	Pinch torque
T_μ	Friction torque
μ_v	Vibration torque
$A, F,$ and Φ	Coefficient matrix in the continuous system and discrete system, respectively
$B, G,$ and Γ	Input coupling matrix in the continuous system and the discrete system, respectively
C, H	Observation matrix in the continuous system and the discrete system, respectively
w	Plant noise
v	Observation noise
u	System input
$x, x(k)$	State variables in the continuous system and the discrete system, respectively
$y, y(k)$	Observation variables in the continuous system and the discrete system, respectively
T_s	Sample time
$P(k k-1)$	Covariance matrix of prior estimation.
$P(k k)$	Covariance matrix of posterior estimation
$K(k)$	Kalman gain
Q	Plant noise variance
R	Observation noise variance
\cdot	Denotes derivative
$\hat{\cdot}$	Denotes an estimated value

References

- Baker, R.; Coenen, P.; Howie, E.; Williamson, A.; Straker, L. The musculoskeletal and cognitive effects of under-desk cycling compared to sitting for office workers. *Appl. Erg.* **2019**, *79*, 76–85. [[CrossRef](#)] [[PubMed](#)]

2. Vancampfort, D.; Stubbs, B.; Smith, L.; Gardner, B.; Herring, M.P.; Firth, J.; Koyanagi, A. Correlates of sedentary behavior among community-dwelling adults with anxiety in six low- and middle-income countries. *Psychiatry Res.* **2019**, *273*, 501–508. [[CrossRef](#)]
3. Foley, J.T.; S monarson, A.F.; S monarson, H.P.;  gisson, L.F.; Goethe, A.P. Adjust desk-An adjustable height desk. *Matec Web Conf.* **2017**, *127*, 01002. [[CrossRef](#)]
4. Du, Y. The Design of Anti-pinch Window Lifter Based on Double Hall Sensor. Master’s Thesis, Donghua University, Shanghai, China, 2014.
5. Lee, D.H.; Kim, B.W.; Choi, J.K. Model Based Design and Validation of Vehicle Safety Power Window Control Systems. *Trans. Korean Inst. Electr. Eng.* **2010**, *59*, 2298–2305.
6. Liu, J.; Fu, H.; Rao, Z.; Zhao, Y. Anti-pinch Algorithm for Electric Window Based on Gauss-filtering and Approximate Integration. *Automot. Eng.* **2017**, *39*, 1464–1471.
7. Wang, Y.; Qiu, Y. A low-cost anti-pinch control system for electrical window. In Proceedings of the Fourth International Conference on Information & Computing IEEE, Phuket Island, Thailand, 25–27 April 2011.
8. Wibowo, W.K.; Jeong, S.K.; You, S.S.; Jaemin, L. Automatic Threshold on Current based Anti-pinch Mechanism for Power Windows. *Int. J. Electr. Comput. Eng.* **2018**, *8*, 2172–2179. [[CrossRef](#)]
9. Shen, T.; Wu, Z.; Zhu, Y. The Explore of Algorithm About the Anti-pinch of Window Based on Current Detection. *Mechatronics* **2012**, *9*, 40–43.
10. Lee, H.J.; Ra, W.S.; Yoon, T.S.; Park, J.B. Practical pinch detection algorithm for the low-cost anti-pinch window control system. In Proceedings of the IEEE International Conference on Industrial Technology, Hong Kong, China, 14–17 December 2005.
11. Park, J.H.; Ra, W.S.; Park, J.B.; Yoon, T.S. Real-Time Pinch Detection Algorithm: Robust to Impulsive Noise. *Int. J. Control Autom. Syst.* **2009**, *7*, 185–192. [[CrossRef](#)]
12. Yu, X.; Miao, C.; Yang, H.; Li, H.; Liu, F.; Meng, Y.; Chen, H. LMI-Based Method of Robust Fault Detection H_∞ Filter for Anti-Pinch of Pure Electric Vehicles. *Res. J. Appl. Sci. Eng. Technol.* **2012**, *4*, 2555–2653.
13. Zhang, Y.; Zhang, Y.; Ai, Z.; Feng, Y. Study on Electric Sunroof Pinch Detection of Cars Based on Model Reference Adaptive Cholesky Decomposition Filter. *IEEE Trans. Transp. Electrification* **2018**, *4*, 190–201. [[CrossRef](#)]
14. Cao, Z.; Li, Y.; Wang, S.W. Anti-pinch Window Lifter System Based on Kalman Filter with Real-Time Estimation of Measurement Noise. *J. East China Univ. Sci. Technol.* **2015**, *41*, 379–383, 411.
15. Ai, Z.; Zhang, Y.; Zhang, Y.; Feng, Y. Smart Pinch Detection for Car’s Electric Sunroof Based on Estimation and Compensation of System Disturbance. *Control Syst. Eng.* **2018**, *2*, 1–12. [[CrossRef](#)]
16. Sun, D.; Lu, R.; Mills, J.K.; Wang, C. Synchronous tracking control of parallel manipulators using cross-coupling approach. *Int. J. Robot. Res.* **2006**, *25*, 1137–1147.
17. Hua, S.; Ling, Z.; Bin, H. Federated H_∞ Filtering Algorithm and Its Application in Integrated Navigation System. *J. Data Acquis. Process.* **2003**, *18*, 418–422.
18. Jiang, C.; Zhang, S.; Zhang, Q. A New Adaptive H-Infinity Filtering Algorithm for the GPS/INS Integrated Navigation. *Sensors* **2016**, *16*, 2127. [[CrossRef](#)] [[PubMed](#)]
19. Liu, F.; Li, H.; Chen, H.; Meng, Y. Robust fault diagnosis for anti-pinch of pure electric vehicles based on H-/ H_∞ approach. *Appl. Res. Comput.* **2011**, *28*, 4231–4239.
20. Zhao, L.; Wang, X.; Xue, H.; Xia, Q. Design of unscented Kalman filter with noise statistic estimator. *Control Decis.* **2009**, *24*, 1483–1488.
21. Peng, S.; Chen, C.; Shi, H.; Yao, Z. State of Charge Estimation of Battery Energy Storage Systems Based on Adaptive Unscented Kalman Filter With a Noise Statistics Estimator. *IEEE Access* **2017**, *5*, 13202–13212. [[CrossRef](#)]
22. Carvalho, C.M.; Johannes, M.S.; Lopes, H.F.; Polson, N.G. Particle Learning and Smoothing. *Stat. Sci.* **2010**, *25*, 88–106. [[CrossRef](#)]
23. Urteaga, I.; Bugallo, M.F.; Djurić, P.M. Sequential Monte Carlo methods under model uncertainty. In Proceedings of the IEEE Statistical Signal Processing Workshop (SSP), Palma de Mallorca, Spain, 26–29 June 2016; pp. 1–5.
24. De Jesus Romero-Troncoso, R. Multirate signal processing to improve FFT-based analysis for detecting faults in induction motors. *IEEE Trans. Ind. Inf.* **2016**, *13*, 1291–1300. [[CrossRef](#)]
25. Atoui, I.; Meradi, H.; Boulkroune, R.; Saidi, R.; Grid, A. Fault detection and diagnosis in rotating machinery by vibration monitoring using FFT and Wavelet techniques. In Proceedings of the International Workshop on Systems, Signal Processing and their Applications (WoSSPA), Algiers, Algeria, 12–15 May 2013.

26. Zhang, W.; Guo, H.; Wang, Y.; Liu, Y. Research on the Application of Wavelet Analysis in Fault Detection. *Adv. Mater. Res.* **2013**, *756–759*, 468–471. [[CrossRef](#)]
27. Mallat, S.; Hwang, W.L. Singularity detection and processing with wavelets. *IEEE Trans. Inf. Theory* **1992**, *38*, 617–643. [[CrossRef](#)]
28. Qin, X.; Pu, Y. Signal Detection and fault diagnosis based on wavelet transform. *J. Cent. South Univ. Technol. (Nat. Sci.)* **2002**, *33*, 434–437.
29. Sun, Q.; Tang, Y. Singularity analysis using continuous wavelet transform for bearing fault diagnosis. *Mech. Syst. Signal Process.* **2002**, *16*, 1025–1041. [[CrossRef](#)]
30. Wu, Z.; Yang, S.; Liu, Y. Rotating Machinery Early Fault Diagnosis Method Based on Multivariate Empirical Mode Decomposition. *Chin. J. Sci. Instrum.* **2016**, *37*, 241–248.
31. Liu, C.; Yang, Z.; Shi, Z. A Gyroscope signal denoising method based on empirical mode decomposition and signal reconstruction. *Sensors* **2019**, *19*, 5064. [[CrossRef](#)]
32. Hyvärinen, A.; Oja, E. Independent component analysis: Algorithms and applications. *Neural Netw.* **2000**, *13*, 411–430. [[CrossRef](#)]
33. Dan, S. Optimal State Estimation (Kalman, H_∞ , and Nonlinear Approaches). In *Additional Topics in H_∞ Filtering*; John Wiley & Sons: Hoboken, NJ, USA, 2006.
34. Andrieu, C.; Doucet, A.; Holenstein, R. Particle markov chain monte carlo methods. *J. R. Statist. Soc. B.* **2010**, *72*, 269–342. [[CrossRef](#)]
35. Dan, S. Kalman Filtering. *Embed. Syst. Program.* **2001**, *14*, 72–79.
36. Mercorelli, P. Parameters identification in a permanent magnet three-phase synchronous motor for velocity planning to optimize traction losses in a City-Bus. In Proceedings of the 2013 5th International Conference on Modelling, Identification and Control (ICMIC), Cairo, Egypt, 31 August–2 September 2013; pp. 193–198.
37. He, H.; Lian, X. Automatic matching of anti-pinch car window controller. *Automot. Eng.* **2014**, *36*, 740–745.



© 2020 by the authors. Licensee MDPI, Basel, Switzerland. This article is an open access article distributed under the terms and conditions of the Creative Commons Attribution (CC BY) license (<http://creativecommons.org/licenses/by/4.0/>).